DNA Microarray Analysis Using Smartphone to Detect BRCA-1 Gene

SCHOLARONE™
Manuscripts

DNA Microarray Analysis Using Smartphone to Detect BRCA-1 Gene

Alisha Prasad[1], Syed Mohammad Abid Hasan[1], Steven Grouchy[1], Manas Ranjan Gartia [1]*

[1]Department of Mechanical and Industrial Engineering, Louisiana State University, Baton Rouge, Louisiana 70803, United States

* All correspondences should be addressed to mgartia@lsu.edu

Keywords: Smartphone, paper microfluidics, DNA microarray, point-of-care, BRCA-1, 3D Printed Fluorescence Microscope

Abstract: DNA microarrays are used to examine changes in gene expression of large number of genes simultaneously by fluorescent labeling of the complementary DNAs (cDNAs). The major bottleneck of implementing microarray technology in resource-limited setting lies in the detection instrument used for generating images of spotted oligonucleotides post-hybridization. While various methods such as lateral flow assay have been presented to accomplish point-of-care disease detection, there is no simple and effective instrument available to gather spot images maintaining the standard microarray procedures. Nanotechnology based sensors connected with a portable smartphone readout system has the potential to be implemented for microarray technology. Here, we describe a portable fluorescence microarray based imaging system connected to a smartphone for detecting breast cancer gene expression (BRCA-1) from exon 11. This is based on the interactive binding of probe DNA to Cy3-target DNA. Paper-based microfluidics approach was used to demonstrate the DNA hybridization assay. The imaging principles of the assembled device named "FluoroZen" are similar to a fluorescence microscope. It uses two light spectrum filters, one to excite the fluorescent dye and the second to capture the emission spectrum. The images were acquired by the CCD cameras from the FluoroZen. Smartphone integrated paper microfluidics platform presented here could be translated into clinical settings to perform point-of-care testing.

INTRODUCTION

With the increasing demand and pressure on health care budgets, progressive global initiatives have been undertaken to make healthcare more patient centered, reliable, available, and affordable. Self-monitoring pregnancy and diabetes kit are by far the largest testaments of point-of-care (POC) devices.[1] This motivates to bridge the gap by building more POC devices to allow monitor and control all aspects of healthcare in real time. In the last few years the advances in science and technology has facilitated various POC devices for portable diagnosis of diseases, food safety and quality control,[2] environment monitoring,[3, 4] animal diagnostics pathogen detection,[5, 6] and endemic inspection in remote areas.[7] Statistics reveals that the use of POC devices is gradually increasing in the United States, with anticipated growth rates of >15% in the coming years.[8] The advantage of POC

devices are that they allow to perform the tests onsite and share the information *via* e-texts, cloud computing services, and GPS.[9, 10] Point-of-care-testing (POCT) has opened doors for personalized diagnosis, making healthcare more accessible with prompt clinical decisions resulting in improved patient safety and overall patient satisfaction.[11, 12] The turnaround time (TAT) to generate on-site test results are a major advantage of POC devices. The ability to perform on-site detection along with incorporation of platform technology has helped to expedite medical decision-making process translating clinical interventions and ultimately benefiting patient and improving life.[13]

The rapid development of smartphone technology with increasing computing power, high resolution cameras, geo positioning system (GPS) capabilities and internet connectivity has enabled smartphone-based POCT platform suitable for field deployment.[14, 15] Smartphone-built-POC devices have been so far utilized as stethoscopes,[16] integrated with ultrasound instrument,[17] used as brightfield-microscopes,[18] used as fluorescence microscopes,[19] applied as spectrometer for biosensing, [20] and colorimetric based assay instruments.[21] Recently, fluorescence-based detections of chemically tagged analytes with smartphone readout platforms have been demonstrated as a robust method with high sensitivity and specificity to address various biological assays.[22-24]

Despite the introduction of DNA hybridization assay since 1980's,[25] several approaches have been established with an attempt to simplify the hybridization assay by immobilization of the probes[26] from standard pin-spotting to robotic system deposition,[27] laser writing,[28] electrospray deposition,[29] inkjet printing,[30] etc. Existing methods of DNA hybridization rely mostly on conventional microscope slides.[31] Literature reveals that DNA microarrays have also been explored using nanostructured photonic crystal (PC) substrates.[32] While various methods have been reported on DNA hybridization, there is little-to-no-literature on the instruments required to detect these spotted oligonucleotides. A major limitation associated with it is costly instrumentation and the laboratory-controlled setting adding to the complexity and fragility to detect hybridized arrays. Furthermore, such instruments require assistance of a well-trained staff which further leads to delay in diagnosis, increase in the turnaround time and eventually affecting healthcare.[33, 34] The introduction of paper-based microfluidic systems (µPADs) by *Whitesides* group[35] emerged as a promising technology as an inexpensive, flexible, biodegradable platform to address the growing need of POCT in resource-limited settings.[36, 37] Recently, their group also described a new method for accumulating both proteins and nucleic acids on paper. They demonstrated its utility for bio sensing by binding it with antibodies or complementary nucleic acids to create protein or DNA arrays using µPADs .[38] Hence, the integration of µPAD technology for biological assays with smartphone readout system can be helpful as it will provide: (i) reliable, rapid and cost effective analysis, (ii) reduce TAT, (iii) provide onboard processing abilities to share data, and (iv) ultimately provide means for POC diagnostic devices.[39, 40]

Several smartphones based platforms have been reported for biological assays such as to perform Enzyme Linked Immunosorbent Assays (ELISA) for protein biomarker detection,[14] use as microplate based ELISA,[41] for herbicide detection,[42] Loop Mediated Isothermal Amplification (LAMP) assay performed on microfluidics and smartphone-based readout to detect DNA,[43] for quantitation of food toxins,[44] for protein immunoassays,[45] and protein detection.[46]

Here, we present DNA hybridization coupled with a smartphone based readout system. We assembled a POC device which we named "FluoroZen" to perform optical assessment of DNA hybridization assay by detecting the fluorescent oligonucleotide spots on the nitrocellulose (NC) paper. The device is made of two types of filters: (i) excitation filter, to narrow the excitation light of the light-emitting diode (LED) projected on the spots, and (ii) emission filter for visualizing the fluorescent spots. Other components include a standard glass slide holder (75 x 25 x 1 mm³), an ON/OFF switch, and an adjustable smartphone holder. The device and its components were designed in SolidWorks and fabricated using 3D-printing technology. FluoroZen works on a principle similar to the fluorescence microscope where the spots with higher intensity will give brighter spots than the others. Here, we report a versatile DNA microarray platform for detecting breast cancer gene expression (BRCA1) from exon 11.[47] We chose BRCA1 gene, firstly due to its high prevalence in half of the global population, and secondly because, a lot of researched data about the alterations and mutations are available at the gene level from various databases. These collective source information, was our base point to design invariable number of primers and its complementary oligonucleotides, for building a paper based DNA microarray platforms for POCT. The measurement of cancer-related biomarkers might provide valuable prognostic information for possible metastatic risk. Disease specific DNA hybridization assay is based on the interactive binding of DNA to Cy3- labelled cDNA. The assay was based on the capillary transfer of DNA molecules immobilized in a certain microvolume.[48] The hybridization was achieved when the probe DNA interacts with a specific labelled target DNA while the non-hybridizing DNA was eliminated by capillary forces upon washing. The images were acquired by the CCD cameras from the FluoroZen. Utilizing paper microfluidics for biological assays along with the smartphone readout setup presented in this work opens up the possibility of transferring various clinical tests to POCT.

EXPERIMENTAL SECTION

Materials and Chemicals

DNA oligonucleotides for exon 11 for BRCA1 gene conjugated at one end with Cyanine-3 were designed using NCBI-Primer BLAST and ordered from Sigma Aldrich (St. Louis, MO, USA). Reagents such as Bovine Serum Albumin (BSA) (Sigma), Sodium Dodecyl Sulphate (SDS) (Sigma), and Saline Sodium Citrate (SSC) (Sigma) were utilized as received. Phosphate Buffer Saline (PBS), and Whatman No.1 filter paper (11 µm pore size) was

supplied from Biorad Laboratories, USA. The deionized (DI) water from a Milli-Q water purifying system was used throughout the experiments. Excitation filter (XF1074 525AF45) with 22 mm clear aperture and Emission filter (XF3085 565ALP) with 15 mm clear aperture were purchased from Omega Opticals (Brattleboro, VT, USA). 3.4 V-5 mm Round LEDs (480-570 nm wavelength), 1-ohm resistor, AAA-batteries, and 3D printing 1.75 mm PLA filament were ordered from Amazon (Amazon.com).

Paper Microfluidics

The pressure driven fluid flow in paper microfluidics was evaluated by designing channels using AutoCAD 2016 followed by printing (Xerox ColorQube 8580/N Wax Printer, Xerox Corporation, USA), and baking (at 120° C for 2 minutes) in the oven (Quincy Lab 20GC Gravity Lab, USA) to spread the molten wax in NC filter paper (**Fig. 1a**). The difference in fluid flow before and after baking was demonstrated and the scanning electron micrographs of the different regions was also procured. The interplay between the channel dimensions with the sample volume was conducted to find an optimal design to carry out the DNA microarray experiment. The Resolution of the printing and baking system was evaluated using USAF Resolving Power Test Target 1951 by printing and baking a standard 3 x 3 inches^2 and 2 x 2 inches^2 (visualizing Group numbers 2 to 3), and 20 x 20 mm^2 and 15 x 15 mm^2 (visualizing Group numbers 4 to 5) negative test pattern.

Smartphone Readout Setup

A portable optical sensing setup termed "FluoroZen" was made for detecting cancer biomarkers. The device was supported with excitation and emission filters operating within 520-575 nm wavelength range to gather, collimate, and disperse light. A green LED light was used to project through the excitation filter inclined at 30° and stationed at 35 mm working distance from the sample area. The sample area was illuminated at 90° along the light collection axis visualized through the emitter filter and images were captured by the smartphone placed on the top. In order to block external light and limit diffraction, the entire device was printed black. All the images in this study were acquired using the built-in camera of the smartphone (8-megapixel, iPhone 6). Image J software was used to deduce the RGB (Red, Green, Blue) pixel value corresponding to the intensities retrieved from the image of the sample spot area. As our operating filters lie within the visible spectrum of 400-700 nm regime, we evaluated auto-fluorescence of FluoroZen by introducing Cy3-dye on wax printed and baked iconic images, and adding orange colored food dye on a tiger imprint. Furthermore, LSUTIGER labelled with different colored letters were also printed to find the color with maximum auto-fluorescence. Limit-of-Detection (LOD) of the device was estimated from image sets of arrays with various concentrations of Cy3-DNA oligonucleotide probes from 0-10 µM made by serial dilution with 3X SSC buffer and a control background (just 3X SSC buffer). The experiment was performed in triplicates for each set.

DNA Hybridization Assay

The utility of FluoroZen as a proof-of-concept platform for optical sensing applications, was demonstrated by the DNA Microarray (or DNA hybridization) experiment for detection of breast cancer specific gene expression (BRCA1). 20 bp short oligonucleotide primers specific to Exon 11 of BRCA1 were used in our experiments. The different DNAs are labelled as probe DNA(T); target DNA (perfectly matched oligonucleotide (BRCA1 (+))); non- cDNA (as negative control (BRCA1(-)); and 2-base pair mismatched DNA (for specificity (BRCA1(Mis)). Except the probe DNA (hereafter called "DNA-1"), all the remaining DNAs were conjugated with Cy3 dye (hereafter called "DNA-2"). The working concentration of the probe DNA was 10 µM prepared from 100 µM stock concentration by dilution with 3X SSC buffer. The DNA hybridization assay consisted of four main steps, (i) Loading DNA-1, (ii) Blocking, (iii) Loading DNA-2, and (iv) Washing. First, 1 µL of DNA-1 was dropped into the inlet zone with ~25 seconds wait time until it reached the RZ (Reaction Zone). Second, 1% BSA/PBS was added for blocking the unbound DNA and left approximately for 15 minutes until dry. Third, 1 µL of DNA-2 was dropped from the same inlet with ~60 seconds wait time until it reached the RZ for hybridization. Finally, 3 µL of 1% SDS was added slowly for washing and removing the unhybridized DNAs until it reached end of the channel. The buffer was heated at 37° C prior to use to avoid SDS precipitation. Each set of experiment took nearly 20 minutes and 3 sets of experiments were performed for each pair. The experiments were performed in minimal light exposure to avoid photobleaching. Images were captured immediately from FluoroZen by an Apple iPhone 6 by placing the completely dried test run paper on the glass slide chamber, followed by image analysis using Image J software as mentioned previously.

RESULTS AND DISCUSSION

Paper Microfluidics

The nature of guided capillary flow in paper microfluidics was demonstrated by introducing different colored food dyes in individual channels before and after baking as shown in **Fig. 1c**. Upon baking, the molten wax penetrated into the paper creating a confined channel for guided flow of the individual colors orange, red, green, and blue respectively, while for non-baked channels the colors merged and smeared all over. The acquired SEM images in top (**Fig. 2a**), and cross-sectional view (**Fig. 2b**) showed a wax print block on a NC paper wherein the cellulose fibers remained intact and unchanged. **Fig. 2c and 2d** revealed that adding food dye did not alter the fiber property. But in case of baked channels **(Fig. 2e-f)**, the molten wax created hydrophobic barriers and the fibers were conjoined, while fibers are disjoined in the regions where wax is absent, indicating hydrophilic region. µPADs are built on the concept of isotropic process and since every printing and baking system has its own settings there is a limit in the resolution that can be obtained from the system.[49] Hence, in order to overcome this ambiguity, all the parameter settings (thickness and porosity of the paper, orientation of fibers, line width, temperature and time of baking) should be consistent throughout the experimentation. A similar study established from George Whiteside's group in understanding wax printing before and after baking was adapted to

understand our settings and deduce a mathematical expression based on our system.[50] Single lines with nominal widths from 100-450 µm were printed and the degree of spreading of wax in paper was assessed after baking. The linear fit yielded $W_b = 1.01 W_p + 120$, $R^2 = 0.99$. where, W_b = Barrier width, and W_p = Printed Width **(Fig. S1)**. Two lines with nominal widths from 20-350 µm were printed to evaluate the minimum space that can be created using two channels with both white and black background. The linear fit for white background yielded $S_b = 0.95 S_p - 65$, $R^2 = 0.99$. (S_b = Barrier space, S_p = Printed space) **(Fig. S2)**. The linear fit for black background yielded $S_{b\ (black\ BG)} = 0.92 S_{p\ (black\ BG)} - 77$, $R^2 = 0.99$. ($S_{b\ (black\ BG)}$ = Barrier space created with black background, $S_{p\ (black\ BG)}$ = Printed space created with black background) **(Fig. S3)**. Although, there is only a slight difference, in the c-intercept, this value is very important to create precise channels. The hydrophilic and hydrophobic boundaries on the paper are not very sharp which could be resolved by printing patterns on both sides of the paper. Furthermore, these equations could help to predict the final width of hydrophobic barriers and channels and ease the design procedure. For biological studies, controlled fluid flow is important for effective substrate-analyte interaction. For example, in a recent study, wax pillars were made to produce delay barriers to improve the performance and sensitivity of lateral flow assays (LFA). The wax fabricated pillars were further applied for the detection of Human Immunoglobin G (HIgG) and the results showed three times better sensitivity in comparison to the conventional LFA devices.[51] In lieu to this, in the present study, an open channel design for conducting the DNA hybridization study was established by optimizing the volume/area proportion. For the optimized design shown in **Fig. 1d,** it took ~25 seconds for 1 µL of liquid to reach the second reservoir. The diameter of each of the reservoirs were 3mm, length 15 mm, and width 1 mm **(Fig. S4)**. This volume/area proportion and the time lapse parameter is very critical for effective hybridization of the DNA-1 with DNA-2. This is true for our DNA samples suspended in 3X SSC buffer and it might differ based on the viscosity of other samples. Furthermore, this might also depend on the pore size and surface roughness of the NC paper used [38]. Additionally, this design parameter is particularly important as precise sample dilution is critical to achieve chemical reactions in biological assays. We demonstrated this using a paper dilution circuit that mixes equal volumes of 10 µM Cy3-DNA and 3X SSC buffer and allows control over the dilution factor based on the channel design. This dilution factor is dependent on the relative flow rates or the fluidic "resistances" of the two fluids and hence can differ with the fluids used.[52] The concentration of Cy3-DNA relatively decreased from 10 µM to 2.5 µM. **(Fig. S5)**. Hence, design of the channel and the working concentration of the DNAs is important for effective hybridization of targets with their counter probes. The importance of design parameters on fluid flow in paper microfluidics is shown in **(Fig. S6)**.

The resolution of our printing and baking system was obtained using a standard USAF Resolving Power Test Target 1951. From **Fig. 3a** image it is observed that our system is capable of resolving 23.7 µm line pairs (Group 4, Element 5) for the blue highlighted region (from 3 x 3 inches² image area). **Fig. 3c** shows the cross-sectional intensity profile and **Fig. 3d** shows the Full Width Half Maxima (FWHM) extracted from **Fig. 3c** using Image J. For

1
2
3
4
5
6
7
8
9
10
11
12
13
14
15
16
17
18
19
20
21
22
23
24
25
26
27
28
29
30
31
32
33
34
35
36
37
38
39
40
41
42
43
44
45
46
47
48
49
50
51
52
53
54
55
56
57
58
59
60

2X2 inches^2 image area, the resolution was found to be 32.1 μm (Group 4, Element 4) for the orange highlighted region. **Fig. 3g** shows the cross-sectional intensity profile and **Fig. 3h** shows the FWHM extracted from **Fig. 3g** using Image J.

Smartphone Readout Setup

The image of the smartphone based portable optical sensing platform "FluoroZen" is shown in **Fig. 4**a (Side View) and **4b** (Top View). **Fig. 4c**, shows the different parts and the assembly of the device (image from SolidWorks2016). The schematics in **Fig. 4d**, shows the working principle of FluoroZen. When a sample (containing fluorophores) is illuminated with an LED source the lower energy light emitted at a longer wavelength can be visualized by an emission filter by the naked eye and can also be captured by CCD camera of mobile devices. This is similar to a conventional Fluorescence Microscope, except that it has an interference filter that blocks the unwanted wavelength and efficiently reflects shorter wavelength and projects only the desired band of longer wavelength light.[53] Although this, provides an advantage of multi-modality imaging it increases the cost. FluoroZen, on the other hand, has easy insertion/removal supports to change filter lenses making it both portable and affordable for POCT. The fluorescence property of the device was tested by converting iconic photographs into grayscale text images, followed by printing and baking to impose a facial channel on the NC paper. **Fig. 5a & 5b** shows the procedure as well as the final captured image from FluoroZen upon introduction of Cy3-dye. The bright visible "saffron" color emitted form Cy3 ($\lambda_{emission} \approx 554$ nm) confirms the device capability to detect spectrum within the filters range of 525-565 nm. Hence, the DNA-2 used for our hybridization assay were tagged with Cy3. In order to test whether colored wax would emit fluorescence, the auto-fluorescence property of the microfluidic device was evaluated by printing each letter of "LSUTIGER" using purple, blue, green, red, yellow, orange, black, and pink colors respectively. The image captured using FluoroZen revealed that maximum auto fluorescence was displayed by red colored wax and the least is displayed by green colored wax (red is followed by pink, orange, and yellow colored wax). The colors whose spectrum was closer to the filters spectrum displayed higher intensity and hence were visible by the naked eye, while the remaining were not visible. The colors for each letter were swapped to confirm the auto-fluorescence property **(Fig. 5c)**. The auto-fluorescence property evaluated by adding orange dye on a Tiger imprint reconfirms this as shown in **Fig. 5d**. In order to avoid, discrepancy of auto-fluorescence the optimized channel for the DNA hybridization assay was printed in black (as shown in **Fig. 1c**). In order to find the detection limit and dynamic range of the paper microfluidics based detection system, Cy3-dye was spotted on the paper as shown in the set of images (red channel of the image) in **Fig. 6a.** The intensity of the spot decreases with decrease in concentration such that the fluorescence signals up to a concentration of 0.3 μM could be detected. **Fig. 6b** shows that the fluorescence intensity is linear over at least two-order of magnitude with dynamic range

from 0.1 μM- 10 μM. The LOD was calculated from the limit of blank (LOB) as; LOD = LOB + 1.645 * σ $_{\text{sample with lowest concentration}}$, where, σ = standard deviation, LOB = mean of blank + 1.645 * σ $_{\text{blank}}$. The LOD was calculated to be 0.4 μM corresponding to 400 fmol of dye per zone spotted on the paper. Further the results were compared with spectroscopic based measurement obtained from Cy3, DNA, and Cy3 coupled with DNA samples. The absorbance of the DNA increased with concentration and the peak was found to be ~λ = 260 nm. The absorbance method of detection is reliable up to ~0.6 ng/μL (**Fig. 6d**). The absorbance and emission of the Cy3 is shown in **Fig. 6e** and **Fig. 6c** respectively. The detection limit of fluorescence spectroscopy (**Fig. 6c**) was found to **be 10** times lower than the fluorescence imaging based quantification (~0.04 μM or 40 fmol). The combined absorbance and fluorescence emission data of the dye (**Fig. 6c, 6e, and Fig. S7**) can be utilized to calculate the ratio of number of DNA to dye, which was found to be 8.55 DNA/dye using the following relation:

$$\frac{\text{DNA}}{\text{Cy3 Dye}} = \frac{A_{\text{DNA}} * \varepsilon_{\text{Cy3 dye}}}{A_{\text{Cy3 dye}} * \varepsilon_{\text{DNA}}} \tag{1}$$

where, A = absorbance, and □ = extinction coefficient.

DNA Hybridization Assay

The utility of the device for POC sensing was demonstrated by the DNA hybridization assay.

The optical sensing was based on the signal detection upon interactive binding of DNA-1 with DNA-2. The assay was conducted on our optimized channel design as shown in **Fig. 7a** wherein image set P displayed higher fluorescence in comparison to set M, while set N displayed little-to-no fluorescence. **Fig. 7b** shows the primers for T, BRCA (+), BRCA (-), and BRCA(Mis). The CCD camera of a smartphone was used to acquire the images. The images are then imported to ImageJ software to extract the Red (R), Green (G), and Blue (B) pixel values. The images are converted into 8-bit greyscale images that have 2^8 or 256 intensity graduations in terms of pixels. The pixel with an intensity of 0 is black, while 255-pixel intensity is white and the remaining lies between the shades of grey. The Image J software enables separating pixels which fall within a desired range of intensity values (Region of Interest (ROI)) from those which do not by thresholding (or segmentation). Thresholding is an effective method to measure complex or nonuniform features in an image. The *Analyze* command in Image J software is used to count and measure the thresholded images. The *Analyze* menu also contains a *Set Measurements* dialog box, where in the user can obtain information about the area of selection in pixels, mean gray value, and integrated density *etc*. F**ig. 7c** shows a bar chart for the corresponding fluorescence intensity acquired from the device upon DNA hybridization. The positive sequences (~3.48 X 10⁴) had highest fluorescence intensity in comparison to mismatched (~2.49 X 10⁴) and negative (~1.72 X 10⁴). The intensity from the negative sequences were ~50 % less in comparison to the positive sequences. The low intensity peaks from the

negative sequences might be a resultant of adsorption of residual Cy3 to the NC paper. This optical detection approach provided a semi-quantitative 'YES/NO' response type detection system. The advantage of this approach is that in the microfluidic based approach the hybridization completed in 1 minute compared to long lag time of few hours for the conventional hybridization based assays. Furthermore, use of paper makes it more accessible, affordable, and eco-friendly. The number of DNA copies involved during the hybridization was also calculated based on the assumption that the average weight of 1 base pair (bp) ≈ 660 g/mol using the following formulas:

$$\text{Total number of DNA molecules (g)} = \frac{\text{Molecular weight of DNA template (g/mol)}}{\text{Avogadro's number (molecules/mol)}} \quad (2)$$

$$\text{DNA Copy Number} = \frac{\text{Mass of DNA (g)}}{\text{Total number of DNA molecules (g)}} \quad (3)$$

The total number of DNA copies in 100 µM stock solution was calculated to be 4.705×10^{16} copies in 1.65 mL, where mass of our DNA was 1030.9 µg and the total number of DNA molecules with 20bp length was found to be 2.191×10^{-20} g. For 10 µM working solution and 1 µL working volume used in our assay the initial copy number was found to be 2.85×10^{13} DNA copies. Hence, it can be concluded that a minimum number of 11 log10 DNA copies is required for detecting BRCA-1 genes using the paper microfluidic smartphone readout setup corresponding to 0.4 µM LOD with dilution factor of 250.

CONCLUSION

In summary, a portable optical sensing platform named 'FluoroZen' was developed and demonstrated for detecting BRCA-1 gene breast cancer specific disease biomarker. We presented the fabrication of µPADS on NC filter paper by wax-printing and baking technique.
Based on the standard USAF Resolving Power Test Target 1951 our system is capable of resolving 23.7 µm line pairs. We also deduced three simple equations to predict the final width of printed channels and the hydrophobic barriers, and the space between the channels and lines and ease the design process. Further, a DNA hybridization assay based on paper microfluidics was developed to allow the optical detection of the fluorescent labelled oligonucleotide spots with a semi-quantitative 'YES/NO' response within 20 minutes. Based on the paper-based microarray assay, the LOD of the device was identified to be 400 fmol, with a detection sensitivity of around 11 log10 DNA copies for BRCA-1 genes. In addition, µPADS system are inexpensive, easy to use, and capable of scaling-up. Combining the DNA microarray assay based on µPADS with smartphone readout system is a promising approach to achieve rapid and valuable prognostic information for possible metastatic risks. We envisage extensive use of "FluoroZen" to explore other bioanalytical assays for clinical diagnosis in resource limited settings.

AUTHOR INFORMATION

Corresponding author

* Manas Ranjan Gartia, Telephone: +1-225-578-5900

E-mail: mgartia@lsu.edu

References

1.   J. L. Shaw, *Practical Laboratory Medicine*, 2016, **4**, 22-29.
2.   R. Suebsing, J. Kampeera, B. Tookdee, B. Withyachumnarnkul, W. Turner and W. Kiatpathomchai, *Letters in applied microbiology*, 2013, **57**, 317-324.
3.   R. G. Norkus, J. Maurer, N. A. Schultz, J. D. Stuart, G. A. Robbins and R. D. Bristol, *Chemosphere*, 1996, **33**, 421-436.
4.   M. R. Gartia, B. Braunschweig, T.-W. Chang, P. Moinzadeh, B. S. Minsker, G. Agha, A. Wieckowski, L. L. Keefer and G. L. Liu, *Journal of Environmental Monitoring*, 2012, **14**, 3068-3075.
5.   A. Litster, B. Pressler, A. Volpe and E. Dubovi, *The Veterinary Journal*, 2012, **193**, 363-366.
6.   G. Bansal, W. Zhou, P. J. Barlow, P. S. Joshi, H. L. Lo and Y. K. Chung, *Critical reviews in food science and nutrition*, 2010, **50**, 503-514.
7.   A. Priye, S. W. Bird, Y. K. Light, C. S. Ball, O. A. Negrete and R. J. Meagher, *Scientific Reports*, 2017, **7**.
8.   A. Larsson, R. Greig-Pylypczuk and A. Huisman, *Upsala journal of medical sciences*, 2015, **120**, 1-10.
9.   X. Wang, M. R. Gartia, J. Jiang, T.-W. Chang, J. Qian, Y. Liu, X. Liu and G. L. Liu, *Sensors and Actuators B: Chemical*, 2015, **209**, 677-685.
10. J. Matthews, R. Kulkarni, M. Gerla and T. Massey, *Mobile Networks and Applications*, 2012, **17**, 178-191.
11. K. Mahato, A. Prasad, P. Maurya and P. Chandra, *J Anal Bioanal Tech*, 2016, **7**, e125.
12. P. B. Luppa, C. Müller, A. Schlichtiger and H. Schlebusch, *TrAC Trends in Analytical Chemistry*, 2011, **30**, 887-898.
13. A. St John and C. P. Price, *The Clinical Biochemist Reviews*, 2014, **35**, 155.

14. K. D. Long, H. Yu and B. T. Cunningham, *Biomedical optics express*, 2014, **5**, 3792-3806.

15. K. D. Long, H. Yu and B. T. Cunningham, *Next-Generation Spectroscopic Technologies VIII. Proc. Bellingham, WA: SPIE*, 2015, **98227**, 94820J.

16. G. Comtois, J. I. Salisbury and Y. Sun, 2012.

17. C.-C. Huang, P.-Y. Lee, P.-Y. Chen and T.-Y. Liu, *IEEE transactions on ultrasonics, ferroelectrics, and frequency control*, 2012, **59**.

18. D. N. Breslauer, R. N. Maamari, N. A. Switz, W. A. Lam and D. A. Fletcher, *PloS one*, 2009, **4**, e6320.

19. Q. Wei, H. Qi, W. Luo, D. Tseng, S. J. Ki, Z. Wan, Z. n. Göröcs, L. A. Bentolila, T.-T. Wu and R. Sun, *ACS nano*, 2013, **7**, 9147-9155.

20. D. Gallegos, K. D. Long, H. Yu, P. P. Clark, Y. Lin, S. George, P. Nath and B. T. Cunningham, *Lab on a Chip*, 2013, **13**, 2124-2132.

21. A. W. Martinez, S. T. Phillips, E. Carrilho, S. W. Thomas III, H. Sindi and G. M. Whitesides, *Analytical chemistry*, 2008, **80**, 3699-3707.

22. A. K. Ellerbee, S. T. Phillips, A. C. Siegel, K. A. Mirica, A. W. Martinez, P. Striehl, N. Jain, M. Prentiss and G. M. Whitesides, *Analytical chemistry*, 2009, **81**, 8447-8452.

23. K. Nishi, S.-I. Isobe, Y. Zhu and R. Kiyama, *Sensors*, 2015, **15**, 25831-25867.

24. A. Abbaspour, M. A. Mehrgardi, A. Noori, M. A. Kamyabi, A. Khalafi-Nezhad and M. N. S. Rad, *Sensors and Actuators B: Chemical*, 2006, **113**, 857-865.

25. M. Pollice and H. Yang, *Clinics in laboratory medicine*, 1985, **5**, 463-473.

26. A. Abe, M. Kitagawa, Y. Ikuta, S. Miyakoshi, H. Danbara, N. Kashiwagi and F. Obata, *Journal of immunological methods*, 1992, **154**, 205-210.

27. R. P. Auburn, D. P. Kreil, L. A. Meadows, B. Fischer, S. S. Matilla and S. Russell, *TRENDS in Biotechnology*, 2005, **23**, 374-379.

28. P. Serra, M. Colina, J. M. Fernández-Pradas, L. Sevilla and J. L. Morenza, *Applied physics letters*, 2004, **85**, 1639-1641.

29. B. Lee, A. Tajima, J. Kim, Y. Yamagata and T. Nagamune, *Biotechnology and Bioprocess Engineering*, 2010, **15**, 145-151.

30. C. Lausted, T. Dahl, C. Warren, K. King, K. Smith, M. Johnson, R. Saleem, J. Aitchison, L. Hood and S. R. Lasky, *Genome biology*, 2004, **5**, R58.

31. D. Zhang, J. Lee, M. B. Sun, Y. Pei, J. Chu, M. U. Gillette, T. M. Fan and K. A. Kilian, *ACS central science*, 2017.

32. P. C. Mathias, S. I. Jones, H.-Y. Wu, F. Yang, N. Ganesh, D. O. Gonzalez, G. Bollero, L. O. Vodkin and B. T. Cunningham, *Analytical chemistry*, 2010, **82**, 6854-6861.

33. C. D. Chin, V. Linder and S. K. Sia, *Lab on a Chip*, 2007, **7**, 41-57.

34. J. Wang, *Biosensors and Bioelectronics*, 2006, **21**, 1887-1892.

35. A. C. Siegel, S. T. Phillips, M. D. Dickey, D. Rozkiewicz, B. Wiley, G. M. Whitesides and A. W. Martinez, *Journal*, 2014.

36. A. W. Martinez, S. T. Phillips, M. J. Butte and G. M. Whitesides, *Angewandte Chemie International Edition*, 2007, **46**, 1318-1320.

37. A. W. Martinez, S. T. Phillips, G. M. Whitesides and E. Carrilho, *Journal*, 2009.

38. A. C. Glavan, J. Niu, Z. Chen, F. Güder, C.-M. Cheng, D. Liu and G. M. Whitesides, *Analytical chemistry*, 2015, **88**, 725-731.

39. G. Luka, E. Nowak, J. Kawchuk, M. Hoorfar and H. Najjaran, *Royal Society open science*, 2017, **4**, 171025.

40. F. B. Myers and L. P. Lee, *Lab on a Chip*, 2008, **8**, 2015-2031.

41.   B. Berg, B. Cortazar, D. Tseng, H. Ozkan, S. Feng, Q. Wei, R. Y.-L. Chan, J. Burbano, Q. Farooqui and M. Lewinski, *ACS nano*, 2015, **9**, 7857-7866.
42.   Y. Wang, M. M. Zeinhom, M. Yang, R. Sun, S. Wang, J. N. Smith, C. Timchalk, L. Li, Y. Lin and D. Du, *Analytical chemistry*, 2017, **89**, 9339-9346.
43.   W. Chen, H. Yu, F. Sun, A. Ornob, R. Brisbin, A. Ganguli, V. Vemuri, P. Strzebonski, G. Cui and K. J. Allen, *Analytical chemistry*, 2017, **89**, 11219-11226.
44.   X. Li, F. Yang, J. X. Wong and H.-Z. Yu, *Analytical chemistry*, 2017, **89**, 8908-8916.
45.   A. Venkatesh, T. van Oordt, E. M. Schneider, R. Zengerle, F. von Stetten, J. H. Luong and S. K. Vashist, *Biosensors and Biodetection: Methods and Protocols Volume 1: Optical-Based Detectors*, 2017, 343-356.
46.   F. Wang, Y. Lu, J. Yang, Y. Chen, W. Jing, L. He and Y. Liu, *Analyst*, 2017, **142**, 3177-3182.
47.   M. Lu, S. D. Conzen, C. N. Cole and B. A. Arrick, *Cancer research*, 1996, **56**, 4578-4581.
48.   A. Reinhartz, S. Alajem, A. Samson and M. Herzberg, *Gene*, 1993, **136**, 221-226.
49.   M. M. Thuo, R. V. Martinez, W.-J. Lan, X. Liu, J. Barber, M. B. Atkinson, D. Bandarage, J.-F. Bloch and G. M. Whitesides, *Chemistry of Materials*, 2014, **26**, 4230-4237.
50.   E. Carrilho, A. W. Martinez and G. M. Whitesides, *Analytical chemistry*, 2009, **81**, 7091-7095.
51.   L. Rivas, M. Medina-Sánchez, A. de la Escosura-Muñiz and A. Merkoçi, *Lab on a Chip*, 2014, **14**, 4406-4414.
52.   J. L. Osborn, B. Lutz, E. Fu, P. Kauffman, D. Y. Stevens and P. Yager, *Lab on a Chip*, 2010, **10**, 2659-2665.
53.   C. M. Brown, *Journal of Cell Science*, 2007, **120**, 1703-1705.

1
2
3
4
5
6
7
8
9
10
11
12
13
14
15
16
17
18
19
20
21
22
23
24
25
26
27
28
29
30
31
32
33
34
35
36
37
38
39
40
41
42
43
44
45
46
47
48
49
50
51
52
53
54
55
56
57
58
59
60

List of Figures

calibration curve for absorbance versus concentration). (e) Absorbance spectrum of Cy3 at the concentrations shown in (c).

Fig. 7 DNA Microarray Experiment Using Paper Microfluidics. (a) Fluorescence Intensity w.r.t Cell. (b) DNA sequence list. (c) Bar chart of normalized intensity from highlighted region for different sequences.
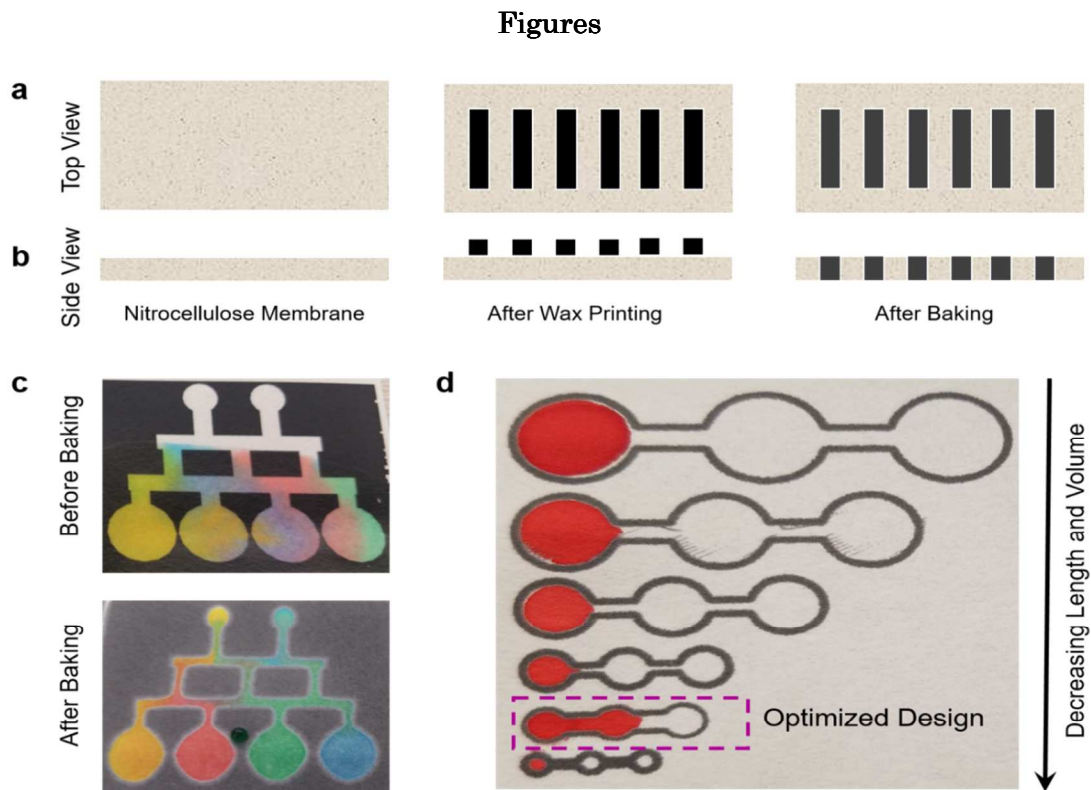
Figures

Fig. 1 Paper-Based Microfluidics. (a-b) Schematics of working principle. (c) Demonstration of fluid flow using food color. (d) Optimization of the design for DNA Microarray study.
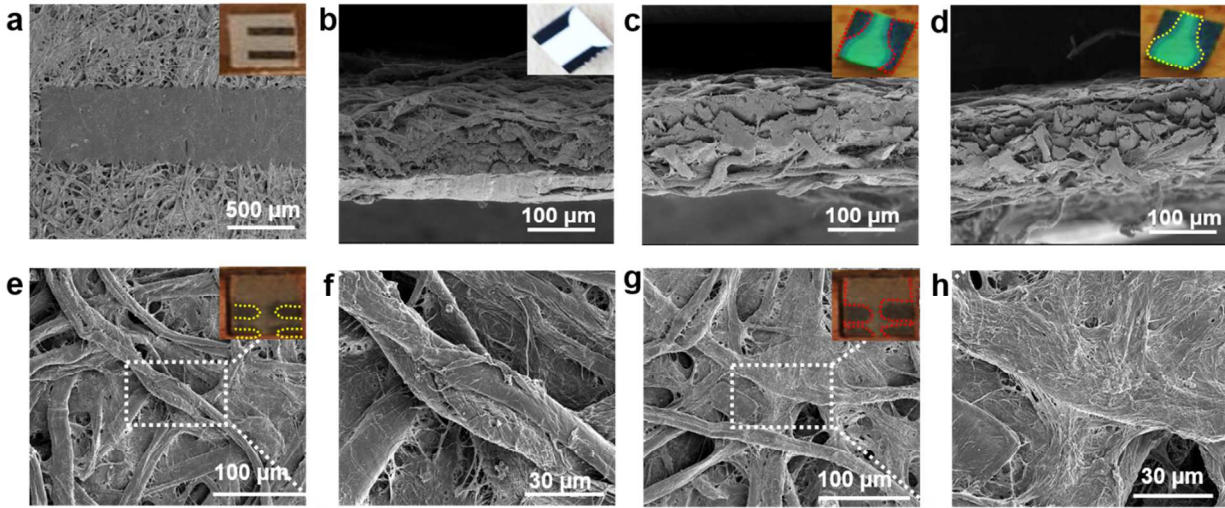
Fig. 2 SEM images. (a-b) After wax printing (as shown in inset). (a)Top View. (b) Cross-sectional View. (c-d) After wax printing and adding dye to the channel. (c) Cross-sectional View of red highlighted region. (d) Cross-sectional View of yellow highlighted region. (e-h) After baking (as shown in inset). (e-f) Hydrophobic barriers created as fibers are conjoined. (g-h) Hydrophilic red highlighted region as fibers are disjoined.
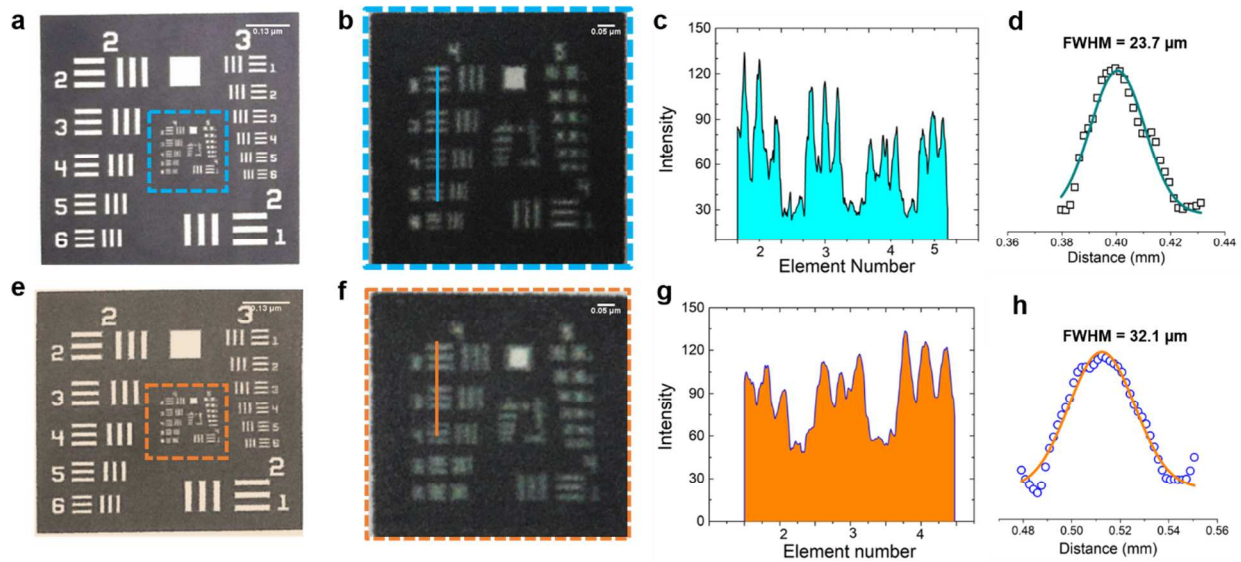

Fig. 3 Resolution of our Printing and Baking system using a standard USAF Resolving Power Test Target 1951. (a) 3 X 3 inches² image area after printing. (b) 20 X 20 mm² blue dotted region of the test target after baking. (c) Cross-sectional profile of Group 4, Element 5, of the resolution target, blue line in (b). (d)FWHM of (c) (e) 2 X 2 inches² image area after printing. (f) 15 X 15 mm² orange dotted region after baking. (g) Cross-sectional profile of Group 4, Element 4, of the resolution target, orange line in (b). (h)FWHM of (g).
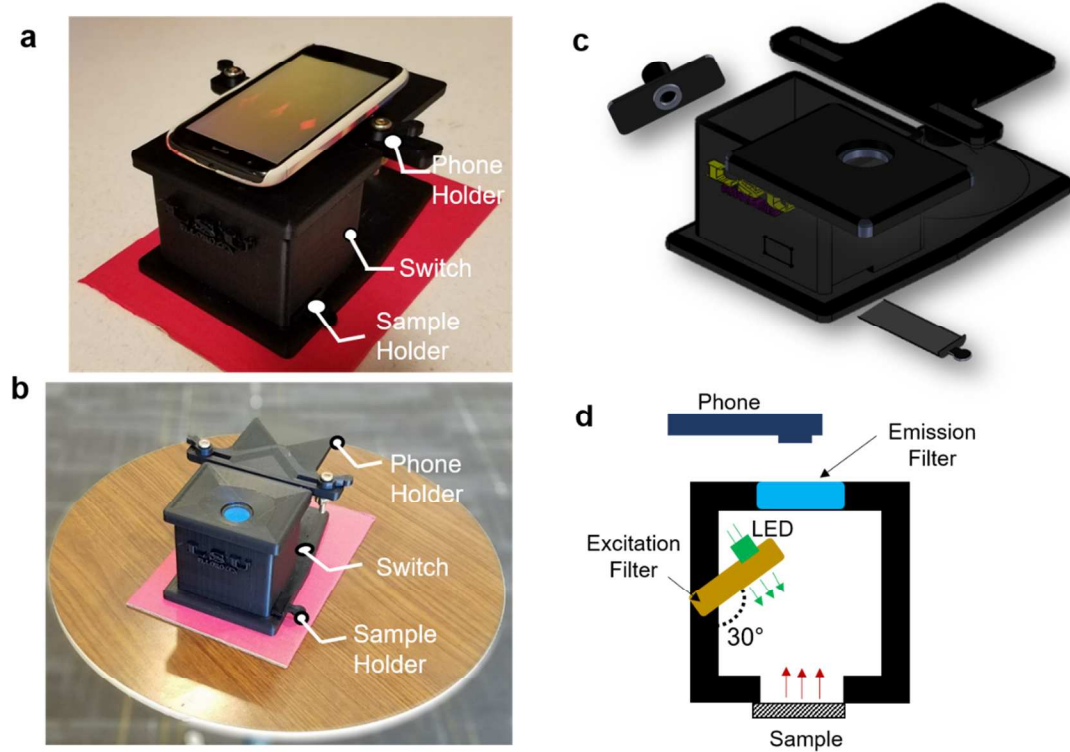
Fig. 4 Optical set up (a) showing the smartphone and the 3D printed platform (b) Optical image of the assembled 3D printed platform. (c) Exploded view of the 3D printed platform showing different components. (d) Schematics of the optical elements of the FluoroZen.

Fig. 5 Evaluating FluoroZen fluorescence property. (a) Image of Abraham Lincoln, (b) standard test image of Lena Soderberg. Left to right: original image, recreation of the image with text in black, after wax printing, after baking, and fluorescence image using FluoroZen. (c) Testing the auto-fluorescence property of the colored wax by printing "LSU TIGER" (top image) and swapping colors (bottom image) for comparison. (d) Fluorescence image of a microfluidic channel created from the image of a tiger.
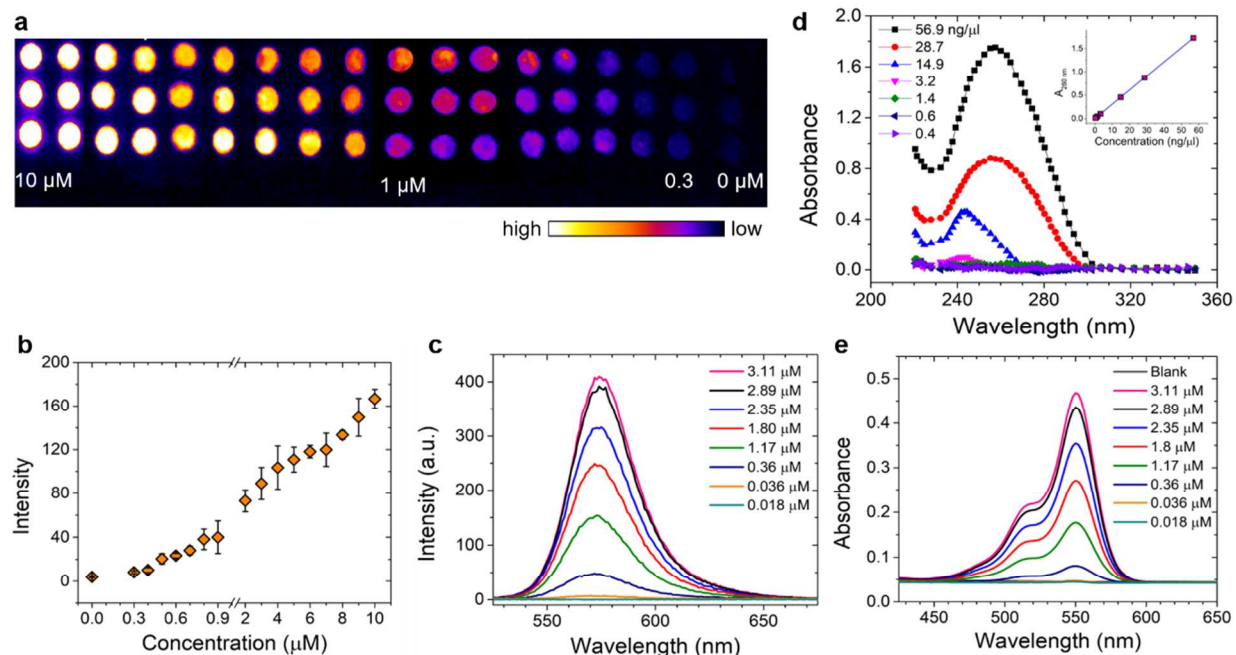
Fig. 6 Limit of detection and dynamic range of paper-based microarray. (a) Image sets of arrays with various concentrations of Cy3-DNA oligonucleotide probes from 0-10 μM and the background (red channel). (b) Variation of fluorescence intensity (RGB pixel value) with concentration of Cy3 in (a). (c) Fluorescence spectrum of Cy3 at different concertation. (d) Absorbance of DNA oligonucleotide at different concertation (inset showing linear calibration curve for absorbance versus concentration). (e) Absorbance spectrum of Cy3 at the concentrations shown in (c).
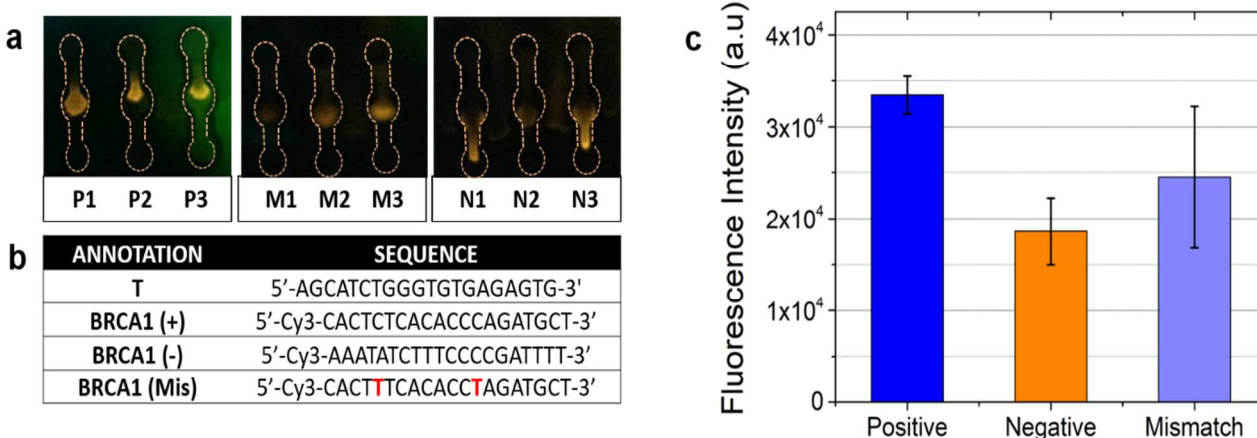

ANNOTATION	SEQUENCE
T	5'-AGCATCTGGGTGTGAGAGTG-3'
BRCA1 (+)	5'-Cy3-CACTCTCACACCCAGATGCT-3'
BRCA1 (-)	5'-Cy3-AAATATCTTTCCCCGATTTT-3'
BRCA1 (Mis)	5'-Cy3-CACTTTCACACCTAGATGCT-3'

Fig. 7 DNA Microarray Experiment Using Paper Microfluidics. (a) Fluorescence Intensity w.r.t Cell. (b) DNA sequence list. (c) Bar chart of normalized intensity from highlighted region for different sequences.

Graphical Abstract for

DNA Microarray Analysis Using Smartphone to Detect BRCA-1 Gene

Alisha Prasad[1], Syed Mohammad Abid Hasan[1], Steven Grouchy[1], Manas Ranjan Gartia[1]*

[1]Department of Mechanical and Industrial Engineering, Louisiana State University, Baton Rouge, Louisiana 70803, United States

* All correspondences should be addressed to mgartia@lsu.edu

Graphical Abstract